Available online at www.sciencedirect.com
ScienceDirect
Remote Sensing of Environment xx (2007) xxx–xxx
Remote Sensing of Environment
www.elsevier.com/locate/rse

Assimilation of remotely sensed data for improved latent and sensible heat flux prediction: A comparative synthetic study

R.C. Pipunic *, J.P. Walker, A. Western

Department of Civil and Environmental Engineering, The University of Melbourne, Parkville Vic. 3010, Australia

Received 12 September 2006; received in revised form 31 January 2007; accepted 4 February 2007

Abstract

Predicted latent and sensible heat fluxes from Land Surface Models (LSMs) are important lower boundary conditions for numerical weather prediction. While assimilation of remotely sensed surface soil moisture is a proven approach for improving root zone soil moisture, and presumably latent (LE) and sensible (H) heat flux predictions from LSMs, limitations in model physics and over-parameterisation mean that physically realistic soil moisture in LSMs will not necessarily achieve optimal heat flux predictions. Moreover, the potential for improved LE and H predictions from the assimilation of LE and H observations has received little attention by the scientific community, and is tested here with synthetic twin experiments. A one-dimensional single column LSM was used in 3-month long experiments, with observations of LE, H, surface soil moisture and skin temperature (from which LE and H are typically derived) sampled from truth model run outputs generated with realistic data inputs. Typical measurement errors were prescribed and observation data sets separately assimilated into a degraded model run using an Ensemble Kalman Filter (EnKF) algorithm, over temporal scales representative of available remotely sensed data. Root Mean Squared Error (RMSE) between assimilation and truth model outputs across the experiment period were examined to evaluate LE, H, and root zone soil moisture and temperature retrieval. Compared to surface soil moisture assimilation as will be available from SMOS (every 3 days), assimilation of LE and/or H using a best case MODIS scenario (twice daily) achieved overall better predictions for LE and comparable H predictions, while achieving poorer soil moisture predictions. Twice daily skin temperature assimilation achieved comparable heat flux predictions to LE and/or H assimilation. Fortnightly (Landsat) assimilations of LE, H and skin temperature performed worse than 3-day moisture assimilation. While the different spatial resolutions of these remote sensing data have been ignored, the potential for LE and H assimilation to improve model predicted LE and H is clearly demonstrated.

Keywords: Latent and sensible heat fluxes; Skin temperature; Soil moisture; Land surface model; Data assimilation; Ensemble Kalman Filter

1. Introduction

The land surface provides a continuous feedback of latent (LE) and sensible (H) heat flux to the atmosphere, which drives our weather and climate. Hence the accuracy of heat flux outputs from land surface models (LSMs) plays an important role in the accuracy of weather and climate forecasts from coupled atmospheric prediction models (Pitman, 2003). LE and H result from the partitioning of available net radiation energy at the land surface, and this feedback is related to a combination of soil moisture content, soil temperature, various soil physical properties, vegetation cover, and physical and biological properties relating to particular vegetation types. LSMs are an attempt to relate these factors in a mathematical framework, together with meteorological variables, for predicting water evaporation from soil and/or its transpiration through vegetation (LE) and conductance of heat (H) to the atmosphere on a continuous time scale. The CSIRO Biosphere Model (CBM) is one such model (Wang et al., 2001) and was used for undertaking the experiments in this study.

Models such as CBM are limited in that they represent highly variable and complex physical systems with simplified and/or

* Corresponding author. Tel.: +61 3 8344 4291; fax: +61 3 8344 6215.
E-mail addresses: r.pipunic@civenv.unimelb.edu.au (R.C. Pipunic), j.walker@unimelb.edu.au (J.P. Walker), a.western@civenv.unimelb.edu.au (A. Western).

0034-4257/$ - see front matter © 2007 Published by Elsevier Inc.
doi:10.1016/j.rse.2007.02.038

empirically derived mathematical relationships. Another shortcoming of LSMs is that they are often overparameterised — there is not enough data on model soil and vegetation parameters to accurately represent the highly variable temporal and spatial variation of these quantities (Crosson et al., 2002; Franks & Beven, 1999; Yates et al., 2003). While field measurements can assist in parameterising models at the point scale with considerable effort (Mertens et al., 2005), accurate parameterisation becomes increasingly difficult when modelling across spatial regions. Model predictions are therefore inherently uncertain, with prediction uncertainty typically increasing through time. Data assimilation is one technique commonly used to correct LSM predictions (e.g. Crosson et al., 2002). This is where observed quantities of a particular variable with known uncertainty are used to adjust predicted model state variables such as soil moisture and temperature, and hence other related quantities such as LE and H at the observation time (Walker & Houser, 2001). The data assimilation process compares the uncertainty in the observation with that in the model prediction to determine the correction required; the data assimilation technique applied in this research is the Ensemble Kalman Filter (EnKF) algorithm (Evensen, 1994).

Many examples exist in literature where data assimilation has been used to improve LSM predictions with efforts mainly focussing on improving soil moisture prediction. An early example by Entekhabi et al. (1994) demonstrates the ability to retrieve the true soil moisture profile of a model from an initial poor guess by assimilating remotely sensed passive microwave and thermal infrared data. The study uses a simplified soil scheme and is a synthetic experiment primarily aimed at testing the assimilation algorithm. Walker &Houser (2001) present a synthetic study on surface soil moisture assimilation motivated by the need to improve soil moisture initialisation for climatological and hydrological predictions. Synthetically generated surface soil moisture observations were assimilated into a catchment based LSM with degraded initial moisture values. Observations were assimilated every 3 days to replicate the temporal scale of surface soil moisture data that would be available from satellite sensors. It is shown that the assimilation could retrieve the true soil moisture content for the entire soil profile. To augment past synthetic studies, Crow & Wood (2003) mention the need to further test assimilation applications using real data to better understand the challenges of data assimilation in an operational context. In their study, airborne measurements of 1.4 GHz surface brightness temperature (equivalent to the data that will be available from the SMOS satellite sensor) were assimilated into a LSM to correct soil moisture predictions. Surface state and flux predictions from assimilation outputs were found to be more accurate than predictions from open loop modelling.

Some early studies (Bouttier et al., 1993; Mahfouf, 1991) have shown that assimilating screen level (2 m above ground) air temperature and relative humidity observations can correct soil moisture for improved numerical weather prediction. Seuffert et al. (2003) assimilated a combination of synthetic 1.4 GHz brightness temperature observations together with screen level air temperature and relative humidity measurements to test the potential for improving soil moisture. Assimilation of all of these variables was shown to result in the greatest improvement in soil moisture and heat flux predictions compared to assimilating the screen level variables or brightness temperature data alone. McNider et al. (1994) showed using two experiments that assimilation of surface skin temperature had a positive impact on model predictions. A one-dimensional experiment was conducted with field measured thermal infrared data from a downward-looking radiometer, and a spatial experiment was performed using GOES satellite thermal infrared observations. A more recent example by Margulis & Entekhabi (2003) examined the assimilation of skin temperature together with screen level air temperature and relative humidity into a coupled land surface-atmospheric boundary layer model with both a synthetic experiment and a one-dimensional application using field measured radiometer data. Again, the results showed that assimilating multiple observation types allowed for more robust estimation of model states and fluxes.

The aim of most of these assimilation experiments was to correct root zone soil moisture prediction and hence indirectly correct the heat flux predictions, but achieving physically correct soil moisture estimates through data assimilation does not guarantee improved heat flux prediction feedbacks to the atmosphere. Consequently, this study tests the hypothesis that assimilation of remotely sensed LE and H observations themselves could potentially produce better heat flux predictions than assimilation of soil moisture observations, or the skin temperature observations from which they are derived. Only one example can be found in literature dealing with LE assimilation (Schuurmans et al., 2003), which shows promising results. However, the results are largely unverified and more research is required to determine if and how well assimilation of LE and H can improve heat flux, soil moisture and soil temperature predictions from LSMs.

Different techniques for estimating LE and H from remotely sensed data have been developed and widely reported in literature over recent years (i.e. Bastiaanssen et al., 1998; Jiang & Islam, 2001; Kustas & Norman, 1996). The energy balance algorithms used to estimate these quantities, such as SEBAL (Bastiaanssen et al., 1998), are based on satellite observations of thermal infrared measurements of skin temperature, available from GOES, MODIS and Landsat sensors. Repeat coverage of these satellites over the same geographical location typically occur twice daily at 1 km resolution for MODIS (morning and afternoon), approximately every fortnight at 30 m resolution for Landsat and hourly at 4 km resolution for the geostationary GOES satellite. These temporal scales for thermal infrared data are best case scenarios, which are unlikely over long periods due to cloud cover. In contrast, the soon to be launched SMOS satellite will provide data at 50 km resolution on a three daily temporal scale irrespective of cloud cover (Kerr et al., 2001). While such variations in spatial resolution are potentially important, this paper presents a synthetic one-dimensional data assimilation study as a proof of concept. Moreover, this study demonstrates the relative impact of LE, H, skin temperature and surface soil moisture assimilation on LSM prediction of LE, H,

Please cite this article as: Pipunic, R. C. et al. Assimilation of remotely sensed data for improved latent and sensible heat flux prediction: A comparative synthetic study. *Remote Sensing of Environment* (2007), doi:10.1016/j.rse.2007.02.038

and root zone soil moisture and temperature, using the typical remote sensing repeat times for the respective data types, ignoring potential cloud impacts.

2. Data assimilation

The original Kalman Filter (KF) is an optimal recursive data processing algorithm first presented by Kalman (1960), and forms the basis for more modern variations such as the EnKF (Evensen, 1994) which was applied in this study. A good introduction to the Kalman filter is presented by Maybeck (1979), and Walker & Houser (2005) provide a review of different data assimilation techniques relating to hydrology, land surface modelling and remote sensing. In terms of land surface modelling, data assimilation aims to use available observations of model variables with known uncertainty to correct model predictions which are not optimal due to a combination of uncertain initial conditions, errors in meteorological forcing data, errors in model physics, and poor knowledge of model parameters.

When applying the KF to non-linear systems, the Extended Kalman Filter (EKF) results. This requires calculation of a tangent linear model which can result in poor state and error forecasts due to model non-linearities. The EnKF overcomes the linearization issue through a Monte Carlo approach, where an ensemble of parallel model runs is generated for the same time period. The model error covariance is then determined from the ensemble spread at the assimilation time step and the ensemble mean taken as the best estimate of the model state. Reichle et al. (2002) present a comparison between the EKF and EnKF in a synthetic soil moisture assimilation study and found the EnKF to be more robust and flexible in covariance modelling, and its performance slightly superior.

The EnKF is one form of a number of direct observer assimilation methods which differs from the EKF only in the way in which model covariances are estimated. It can be summarised as follows:

$$\mathbf{X}_k^a = \mathbf{X}_k^f + \mathbf{K}(\mathbf{Z}_k - \mathbf{Z}_k^f), \tag{1}$$

where subscript k refers to the assimilation time step, superscript f refers to the forecast value and superscript a refers to an analysis (updated) value. The model state vector is denoted by $\mathbf{X}$ and the observation is denoted by $\mathbf{Z}$. The difference between an observed and model predicted value ($\mathbf{Z}_k - \mathbf{Z}_k^f$) is the innovation and is weighted by the Kalman gain ($\mathbf{K}$). Together they determine the correction added to the forecast state vector. In addition to projecting from $\mathbf{Z}$ to $\mathbf{X}$ space, $\mathbf{K}$ is a scaling factor that represents the relative uncertainty of model predicted and actual observations based on the covariance matrices. Therefore

$$\mathbf{K} = \mathbf{P}_k^f \mathbf{H}^T (\mathbf{H}\mathbf{P}_k^f \mathbf{H}^T + \mathbf{R}_k)^{-1}, \tag{2}$$

where $\mathbf{P}$ represents the error covariance of the forecast model states and $\mathbf{R}$ is the error covariance of the observation. The matrix $\mathbf{H}$ is a non-linear operator that relates the state vector $\mathbf{X}$ to the observation $\mathbf{Z}$, with superscript T denoting the matrix transpose. Therefore, if $\mathbf{P}$ is large compared to $\mathbf{R}$ (i.e. observations more trustworthy than model prediction), then $\mathbf{K}$ will approximate to 1 when $\mathbf{X}$ and $\mathbf{Z}$ are the same scalar quantity (i.e. $\mathbf{H}=1$), and the innovation will be relied upon heavily to adjust the forecast states due to the small relative observation error. Alternatively, where $\mathbf{R}$ is large compared to $\mathbf{P}$, $\mathbf{K}$ will approach 0 and the observation will not be trusted sufficiently leaving the final analysis vector $\mathbf{X}_k^a$ relatively unchanged, since the model's forecast is understood to be more reliable in this case.

Implementation of the EnKF in this study can be summarised as follows (Evensen, 1994; Houtekamer & Mitchell, 1998; Walker &Houser, 2005). The background state covariance matrix for determining the model error covariance at assimilation times is defined as

$$P_k^f = \frac{(\mathbf{x}_k^f - \overline{\mathbf{x}}_k^f)(\mathbf{x}_k^f - \overline{\mathbf{x}}_k^f)^T}{m-1}, \tag{3}$$

where $\mathbf{x}$ are individual ensemble members of the state forecast matrix $\mathbf{X}$ and the over-bar represents the ensemble mean across all members. The number of ensemble members is denoted by m. However, explicit calculations of $\mathbf{P}_k^f$ are not actually required and Eq. (1) can be written as

$$\mathbf{X}_k^a = \mathbf{X}_k^f + \mathbf{B}_k^T \mathbf{b}_k, \tag{4}$$

where

$$\mathbf{B}_k^T = \mathbf{P}_k^f \mathbf{H}_k^T, \tag{5}$$

and

$$\mathbf{b}_k = (\mathbf{H}_k \mathbf{P}_k^f \mathbf{H}_k^T + \mathbf{R}_k)^{-1} (\mathbf{y}_k - \mathbf{Z}_k^f). \tag{6}$$

A perturbed observation $\mathbf{y}$ replaces the actual observation $\mathbf{Z}$ in Eq. (1) and is defined as

$$\mathbf{y}_k = \mathbf{Z}_k + \zeta, \tag{7}$$

with ζ being a random observation error term that has zero mean and covariance $\mathbf{R}$. For each observation variable, the typical uncertainty for remotely sensed measurements is used to determine its error range, representing covariance $\mathbf{R}$. Prior to assimilation, a random number generator, which generates numbers with a normal distribution and zero mean is used to generate a single number within this error range which is then added to the observation resulting in a perturbed observation value $\mathbf{y}$. The random number generator is then used again to generate an ensemble of observation values about $\mathbf{y}$ resulting in an observation ensemble with covariance $\mathbf{R}$ (more details on observations are given later). Also

$$\mathbf{H}_k \mathbf{P}_k^f \mathbf{H}_k^T = \frac{\mathbf{q}_k \mathbf{q}_k^T}{m-1}, \tag{8}$$

and

$$\mathbf{q}_k = \mathbf{H}_k (\mathbf{x}_k^f - \overline{\mathbf{x}}_k^f) = (\mathbf{z}_k^f - \overline{\mathbf{z}}_k^f), \tag{9}$$

where $\mathbf{z}$ are individual ensemble members of the perturbed observation and the over-bar denotes the ensemble mean.

Please cite this article as: Pipunic, R. C. et al. Assimilation of remotely sensed data for improved latent and sensible heat flux prediction: A comparative synthetic study. *Remote Sensing of Environment* (2007), doi:10.1016/j.rse.2007.02.038

Hence, it is unnecessary to solve for **H** and therefore **B** can be calculated as

$$\mathbf{B}_k^T = \frac{(\mathbf{x}_k^f - \overline{\mathbf{x}}_k^f)}{m-1}\mathbf{q}_k^T. \quad (10)$$

Therefore calculation of $\mathbf{b}_k$ using Eqs. (6), (7) and (8), and $\mathbf{B}_k^T$ using Eq. (10), then substituting into Eq. (4) will update each individual ensemble member at assimilation time steps. Ensemble generation used the approach developed by Turner et al. (2006-this issue), which is discussed further below.

3. Experiment data and methodology

A synthetic experiment was set up as a proof of concept for the assimilation of remotely sensed LE and H, and intercomparison with the assimilation of skin temperature and surface soil moisture. Synthetically derived observations of LE, H (including a joint combination of LE and H), surface soil moisture and skin temperature were separately assimilated into the CBM forced with data from the first three months of 2003 (January 1 to April 1), and the results compared to see which approach produced the more accurate prediction of LE, H, root zone soil moisture and temperature. Two model scenarios were used in the experiments — a truth scenario where knowledge of meteorological forcing, state initial conditions and parameters is assumed to be perfect, and a degraded scenario which used degraded meteorological forcing, initial conditions and parameters. Fig. 1 shows key soil parameter values used in each scenario. In addition, saturated hydraulic conductivity values of 4.3×10^{-6} ms^{-1} for the truth and 1.1×10^{-5} ms^{-1} for the degraded scenario were applied, as were monthly averaged Leaf Area Index LAI values for January, February and March (0.30, 0.31 and 0.35 for the truth scenario and 0.33, 0.33 and 0.39 for the degraded scenario). All input data required to run the models was taken from the Kyeamba Creek catchment in South Eastern Australia to provide realistic input values. However, the modelling is not intended to represent a particular geographical location.

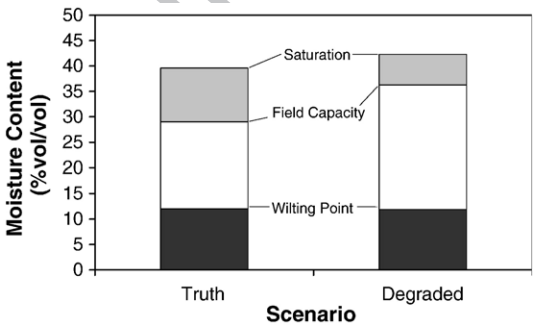

Fig. 1. A comparison between key soil parameter values used in truth and degraded scenarios that were derived from an available catchment data set. Truth values are from a point location and degraded values are catchment area weighted averages.

3.1. The CSIRO Biosphere Model (CBM)

The CBM is a single column model dealing with the exchange of energy, water and CO_2 between a vertical profile represented computationally using six soil layers with uniform soil properties, the land surface, vegetation and the atmosphere (Wang et al., 2001). The thicknesses of the soil layers from top to bottom are 2.2, 5.8, 15.4, 40.9, 108.5 and 287.2 cm respectively with a total soil column thickness of 4.60 m. Each layer has a value for soil temperature and moisture for calculating evaporation, respiration and soil heat flux. Moisture movement through the layers is governed by Richards' equation, the snow scheme is that of Kowalczyk et al. (1994), and a bulk aerodynamic formulation is used to model soil evaporation (Mahfouf & Noilhan, 1991). Amongst the input (forcing) data required to run the CBM are air temperature, downward short and long wave radiation, specific humidity, wind speed, precipitation and barometric pressure.

Four surface types are represented including bare soil, snow (snow does not occur in this study) and a two-leaf canopy model (Wang &Leuning, 1998) which calculates fluxes of LE, H and CO_2 for a 'sunlit' and 'shaded' leaf canopy. A formulation for canopy turbulence is also included based on theory developed by Raupach (1989). Some important vegetation parameters in the model include LAI, canopy height, canopy water storage capacity per unit LAI, average leaf size, the fraction of roots by mass in each soil layer and a number of other parameters related to plant photosynthesis. Vegetation properties for uniform grassland were applied in this study which included typical monthly averaged LAI values for grassland in south eastern Australia and a canopy height of 20 cm. Total values of LE and H calculated by the model represent the respective sums of LE and H for the soil surface and for the vegetation canopy. Using LAI values and a radiation extinction coefficient, the fraction of radiation transmitted through the vegetation canopy is calculated from which LE and H can be calculated for both the soil surface and the canopy.

3.1.1. Model input data

Input forcing data used by this study includes a continuous series of half hourly meteorological data compiled for the Kyeamba Creek catchment from 2000 to present (Siriwardena et al., 2003). It consists of point scale data recorded at the nearest Bureau of Meteorology (BOM) station (Wagga Wagga, ~ 30 km distant) and precipitation data measured at one of the University of Melbourne monitoring sites within the Kyeamba Creek catchment. Given the half hourly temporal resolution of meteorological forcing data, the model was run at half hourly time steps for all of the experiments. Soil parameter data have been estimated by Neil McKenzie (pers. comm., 2005, CSIRO Land and Water Division) based on different soil units across the catchment. These soil units have associated values for field capacity, wilting point, soil bulk density and hydraulic conductivity at saturation, all required as inputs to the CBM. Leaf area index data was sourced from a monthly average, 0.05° by 0.05° spatial resolution publicly available data set derived from remotely sensed Advanced Very High Resolution

Please cite this article as: Pipunic, R. C. et al. Assimilation of remotely sensed data for improved latent and sensible heat flux prediction: A comparative synthetic study. *Remote Sensing of Environment* (2007), doi:10.1016/j.rse.2007.02.038

Table 1
Model forcing variables with associated uncertainty ranges, daily standard errors between truth and degraded values, data type category and values for calculating measurement and offset error standard deviations used in ensemble generation (see Turner et al., in press—this issue)

Forcing variable	Quoted uncertainty	Daily average standard error	Category	h domain	ξ	χ
Short wave radiation (W m^{-2})	±2%	2.2	Semi-restricted	$(0, \infty)$	0.01	0.04
Long wave radiation (W m^{-2})	±3%	3.1	Semi-restricted	$(0, \infty)$	0.003	0.05
Precipitation (mm)	±0.2	0.2	Semi-restricted	$(0, \infty)$	0.2	0.2
Air temperature (°C)	±0.5	0.4	Unrestricted	$(-\infty, \infty)$	0.9	0.4
Wind speed (m s^{-1})	±1.03	0.4	Semi-restricted	$(0, \infty)$	1.0	0.3
Specific humidity (g kg^{-1})	±5%	1.2×10^4	Semi-restricted	$(0, \infty)$	0.0025	0.06

Radiometer visible infrared and near infrared images (Lu et al., 2001).

3.1.2. Truth scenario

The half hourly Kyeamba Creek meteorological data set (Siriwardena et al., 2003) was used directly in its available form for the truth scenario. It includes incoming short wave and long wave radiation, air temperature, wind speed, and specific humidity for the catchment. As no data was available for atmospheric pressure or CO_2 concentration, generic values of 980 mbar and 370 ppm were assigned respectively for the entire time series of the experiment period. Precipitation data used for the truth forcing was sourced from a University of Melbourne monitoring site in the Kyeamba Creek catchment. This location was also used to obtain point estimates of soil and vegetation parameter input into the truth model. Soil moisture content and temperature profiles were not available at the same site for the start of the modelling period (January 1, 2003, 00:30 h). Therefore initial moisture and temperature values were estimated for the six CBM layers based on University of Melbourne data measured at nearby sites for the same time in other years. While arbitrary initial conditions could have been assumed for this synthetic study, these observed quantities were used to provide a set of realistic and internally consistent values.

3.1.3. Degraded scenario

This scenario represents the model prediction results anticipated from the use of erroneous and/or averaged forcing and parameters which is a likely situation when modelling with real data. Hence, spatial input data was averaged within the Kyeamba Creek catchment boundary, or in the absence of spatially distributed data either random perturbations were added (within known uncertainty limits) to the data used in the truth scenario or data was taken from an alternative location within the catchment.

Meteorological forcing inputs were generated by adding random perturbations within determined error ranges to each meteorological data variable used in the truth scenario. The error range for each variable was determined through personal communications with Dr. John Gorman (March 7th, 2006) from the BOM National Climate Centre who is knowledgeable on the typical quality of BOM data. Precipitation was taken from an alternate University of Melbourne monitoring location in the Kyeamba Creek catchment to that used for the truth scenario. Table 1 summarises the error ranges within which the BOM forcing data variables and the University of Melbourne precipitation data were perturbed including the average daily standard error between truth and degraded scenario variables over the 91 day experiment period.

Area weighted averages of available soil and vegetation parameter data within the Kyeamba Creek catchment boundary were calculated for the degraded scenario. Poor initialisation of model states through either lack of data or high uncertainty in the data is a common source of model error which can increase model uncertainty over time, even with accurate forcing and parameters. Initial moisture and temperature values were set to extreme values (higher soil moisture content and lower temperature) compared to the typical summer time values at the start of the experiment period in the truth scenario. This would test the assimilation in a worst case scenario where no information is available to initialise model states. Fig. 2 shows initial soil moisture and temperature value differences between the truth and degraded scenarios, as well as the ensemble ranges.

Fig. 3 highlights the effect of degraded inputs on the truth model. This shows corresponding LE and H outputs from

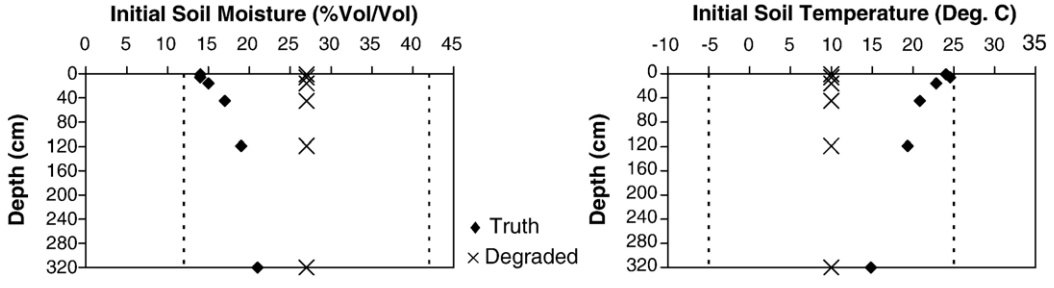

Fig. 2. Truth and degraded scenario initial conditions for soil moisture and temperature. Dashed lines show the minimum and maximum of the ensemble ranges for initial soil moisture and temperature.

Please cite this article as: Pipunic, R. C. et al. Assimilation of remotely sensed data for improved latent and sensible heat flux prediction: A comparative synthetic study. *Remote Sensing of Environment* (2007), doi:10.1016/j.rse.2007.02.038

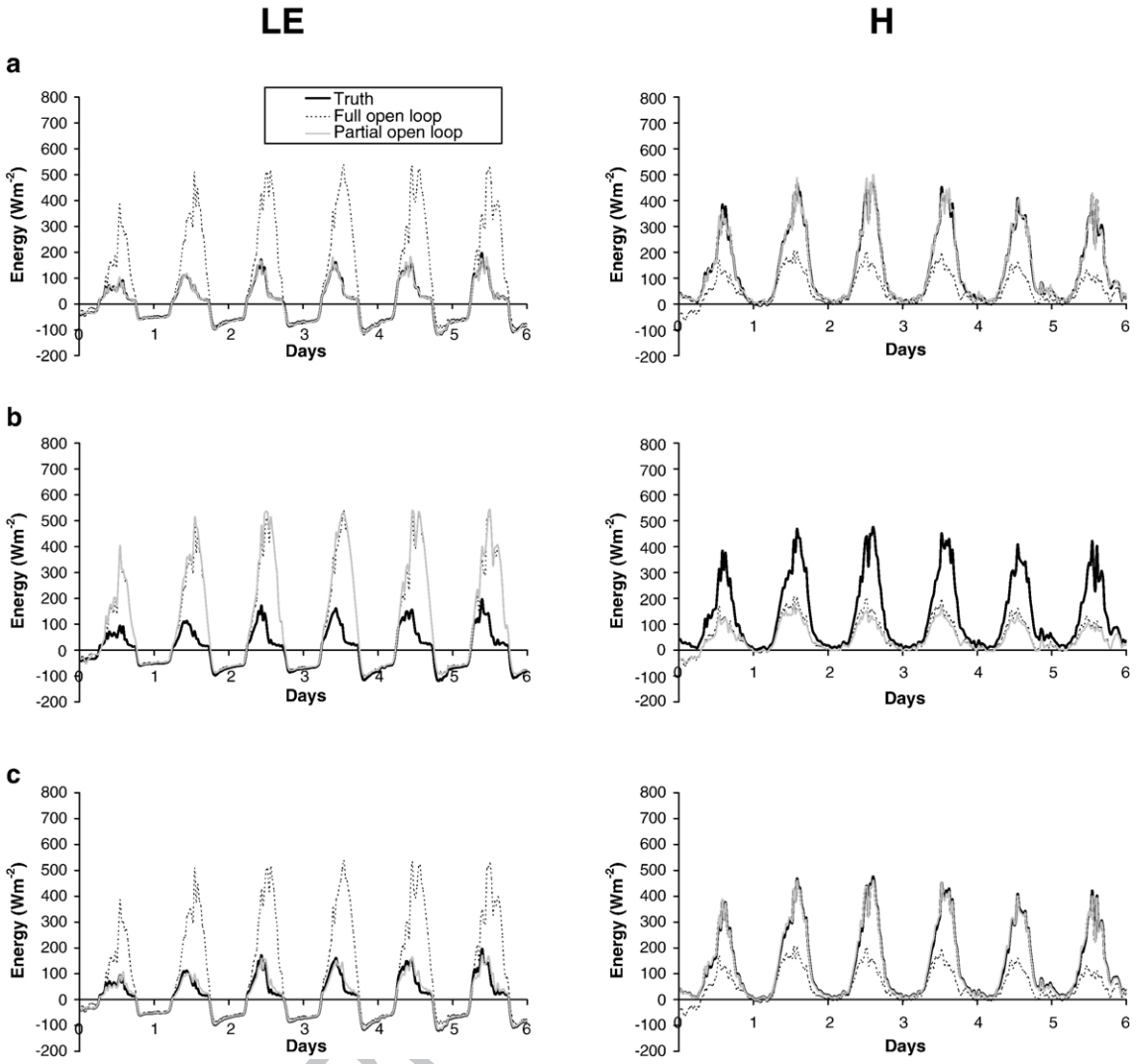

Fig. 3. Outputs of LE and H showing the effect on the truth predictions from 3 separate partial open loop simulations — a) Truth simulation with degraded meteorological forcing, b) Truth simulation with degraded initial conditions, and c) Truth simulation with degraded parameters.

partial open loop simulations resulting from individually using degraded scenario meteorological forcing, initial condition and parameter data into the truth model, with the truth and full open loop (degraded) simulation outputs included for comparison. The degraded forcing and parameters each cause slight but noticeable differences in model output compared to the truth, with degraded parameters having a greater effect on LE than on H. In contrast, the degraded initial conditions cause the greatest deviation from the truth and account for most of the error represented by the full open loop simulation, as they had the greatest uncertainty imposed.

3.2. Synthetic observation data

Truth scenario outputs were sampled at selected time intervals to create synthetic observation data sets of LE, H, joint LE and H, surface soil moisture (from the upper-most 2.2 cm thick soil layer in the CBM) and skin temperature. The time intervals used to sample these variables correspond with the temporal scales of remote sensing platforms that provide information on these quantities (see Table 2). Hence, assimilation of each observation set into the degraded model scenario was intended to emulate the assimilation of available observations.

Two separate observation data sets were created for each of LE, H, joint LE and H, and skin temperature from the truth scenario outputs; twice daily to emulate MODIS observations and fortnightly to emulate observations from Landsat. The top

Table 2
Key characteristics of remotely sensed data types tested in this synthetic study

Observed quantity	Quoted accuracy	Corresponding satellite/sensor	Temporal resolution	Spatial resolution
LE (W m^{-2})	±50	MODIS, Landsat	Twice daily, fortnightly	1 km^2, 30m^2
H (W m^{-2})	±50	MODIS, Landsat	Twice daily, fortnightly	1 km^2, 30 m^2
Surface soil moisture (%vol/vol)	±4	SMOS	Every 3 days	50 km^2
Skin temperature (K)	±2	MODIS, Landsat	Twice daily, fortnightly	1 km^2, 30 m^2

Please cite this article as: Pipunic, R. C. et al. Assimilation of remotely sensed data for improved latent and sensible heat flux prediction: A comparative synthetic study. *Remote Sensing of Environment* (2007), doi:10.1016/j.rse.2007.02.038

soil layer moisture content was sampled once every three days to generate a surface soil moisture observation data set emulating SMOS observations. Uncertainty for remotely sensed estimates of these four variables varies throughout the literature with typical estimates being those given in Table 2 for skin temperature (Kaleita & Kumar, 2000; Sun et al., 2004), LE and H (French et al., 2005), and surface soil moisture (Kerr et al., 2001). These uncertainty ranges were used to prescribe error perturbations to observations and generate observation ensembles during the assimilation experiments. Prior to each assimilation step, a random error value was added to observations within the respective uncertainty range for each observation to generate an observation ensemble as required by the EnKF.

3.3. Model ensemble generation and errors

The EnKF uses an ensemble of model trajectories to represent likely uncertainty in a model prediction. The main sources of error in a model prediction include i) erroneous initial conditions, ii) erroneous meteorological forcing data, and iii) limitations in model physics. The uncertainty in model physics and inclusion of biases has not been treated in this study. Normally distributed random numbers with zero mean and unit variance were generated and used to calculate error perturbations for initial conditions and meteorological forcing data within desired ranges when creating ensembles.

Soil moisture and temperature state initial condition values across the six CBM layers for the degraded scenario were perturbed within a selected range to generate ensembles that reflected the uncertainty in initial conditions. The uncertainty range was chosen such that the true values (i.e. truth scenario initial conditions) were captured within the ensemble (Fig. 2). As a result, degraded scenario initial soil moisture (27% vol/vol) was perturbed with random error within a possible range of ±15% vol/vol, which spans most of the range between wilting point (11.9% vol/vol) and porosity (42.3% vol/vol). The initial soil temperature value (10 °C) was perturbed with random values within ±15 °C for ensemble generation. Generating initial condition ensembles with a large spread about the chosen value is especially important when assimilating with real data if a priori knowledge of initial conditions is poor, as it increases the likelihood of including the true value. The techniques described by Turner et al. (2006-this issue) were employed here to assign random errors to degraded scenario meteorological forcing data and generate each forcing data ensemble, using the parameters specified in Table 1.

4. Results and discussion

Statistically, a greater number of ensemble members results in an ensemble mean and covariance which is closer to reality. However, this comes with increased computation burden. Consequently, it is desirable to use the minimum number of ensemble members while still obtaining a satisfactory estimate of the ensemble mean and covariance. Therefore the first assimilation experiment undertaken was to determine the minimum number of ensemble members required to achieve optimal results from application of the EnKF to the CBM, so as to optimise the computing power available for the subsequent assimilation experiments. An observation data set consisting of once daily LE values sampled from the truth scenario output was used for this purpose, with LE observation errors assigned as in Table 2.

Assimilation over the experiment period with this set of observations was performed separately using five different ensemble sizes — 10, 20, 30, 50 and 100 members. Root mean square error (RMSE) values were calculated between LE outputs from the truth simulation and from assimilation runs performed with each ensemble size to determine an optimal number of ensemble members. Fig. 4 is a plot of the number of ensemble members against RMSE values between LE outputs. The value corresponding to 0 ensembles is the RMSE value between the truth and full open loop outputs for reference. As the declination in RMSE was minimal for more than 20 ensembles, an ensemble size of 20 members was chosen as adequate for carrying out the remaining assimilation experiments.

Fig. 5 shows a series of plots comparing outputs for the first 6 days of the joint assimilation of LE and H twice per day, with that of surface soil moisture once every 3 days. The plots show the initial impacts of the assimilation on four specific CBM outputs — LE, H, root zone soil moisture and root zone soil temperature. Root zone soil moisture and temperature are taken as the average values across the top four soil layers in the model, weighted by each layer's thickness (2.2, 5.8, 15.4 and 40.9 cm), covering a total depth of 64.3 cm.

Based on Fig. 5, heat flux outputs for the first 6 days of the experiment period showed that the twice daily LE and H (proxy for MODIS derived data) assimilation retrieved truth LE and H outputs more quickly and accurately than soil moisture assimilation every 3 days (SMOS observation proxy). The assimilation frequency is the most likely reason for this. However, this is an idealised case that assumes cloud-free conditions. While it is unrealistic to expect twice daily coverage continually, results from the fortnightly assimilation of LE and H (proxy for Landsat derived data) show the corresponding loss of skill that could be expected when extended cloud cover periods exist. In contrast to the LE and H results, it is evident in this initial 6 days that soil moisture assimilation is better than LE and H assimilation for retrieving the true soil moisture, as expected. A reason for this is that LE and H assimilation has a

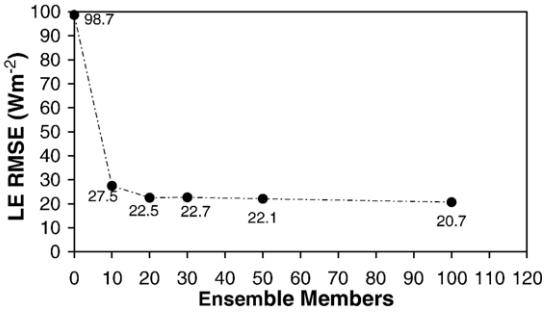

Fig. 4. Ensemble size comparison results for the 91 day experiment period, showing RMSE between truth and assimilated LE outputs for different number of ensemble members.

Please cite this article as: Pipunic, R. C. et al. Assimilation of remotely sensed data for improved latent and sensible heat flux prediction: A comparative synthetic study. *Remote Sensing of Environment* (2007), doi:10.1016/j.rse.2007.02.038

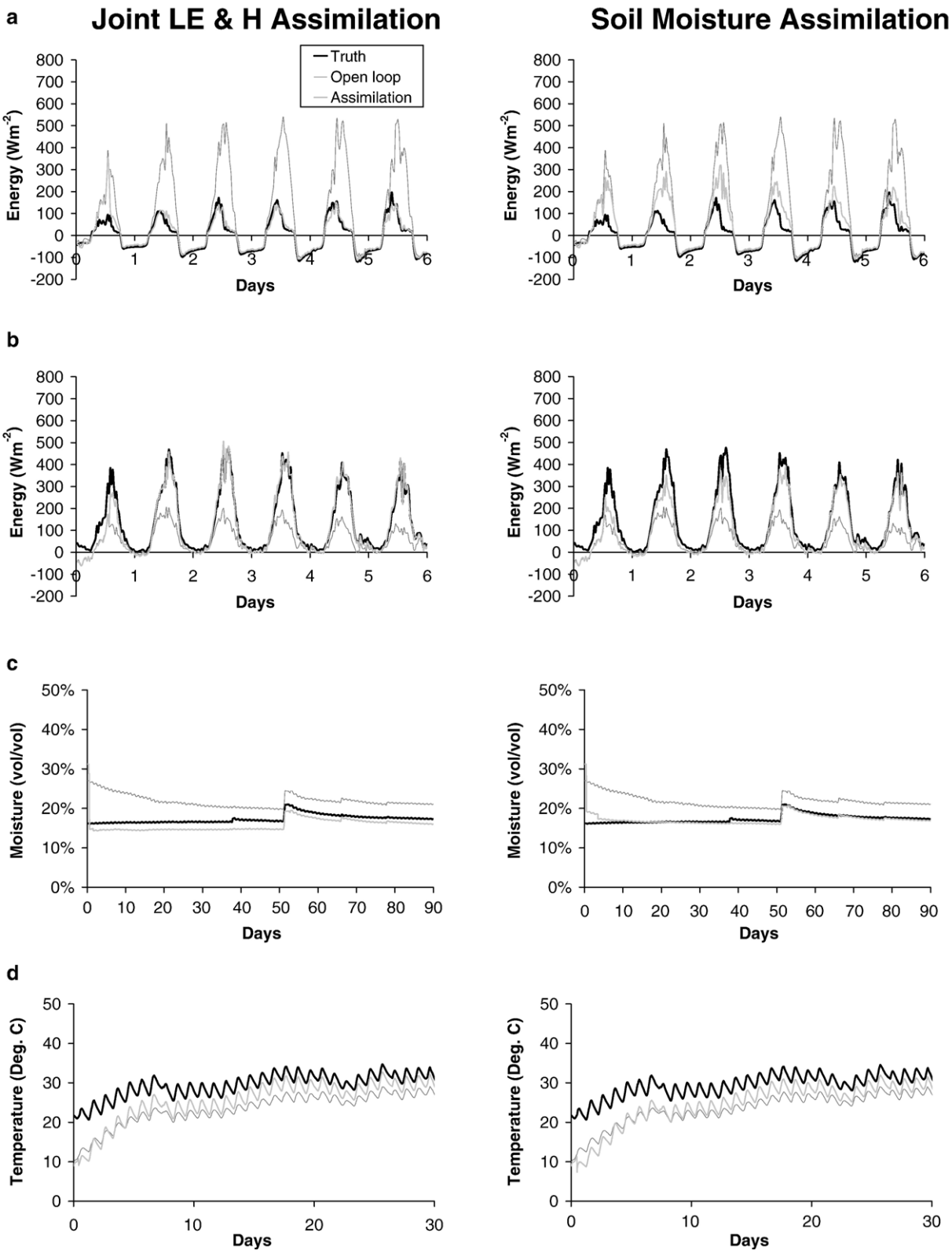

Fig. 5. Outputs from joint LE and H and surface soil moisture assimilation, for estimating a) LE, b) H, c) root zone soil moisture and d) root zone soil temperature.

direct impact on model LE and H, which is used to adjust both soil moisture and temperature states accordingly, whereas assimilating surface soil moisture has a direct impact on the model soil moisture alone. Consequently, the soil temperature is not impacted directly and thus LE and H predictions are initially degraded by soil moisture assimilation.

A full comparison of all the assimilation results over the entire 91 day experiment period is given in Fig. 6, which summarises

Please cite this article as: Pipunic, R. C. et al. Assimilation of remotely sensed data for improved latent and sensible heat flux prediction: A comparative synthetic study. *Remote Sensing of Environment* (2007), doi:10.1016/j.rse.2007.02.038

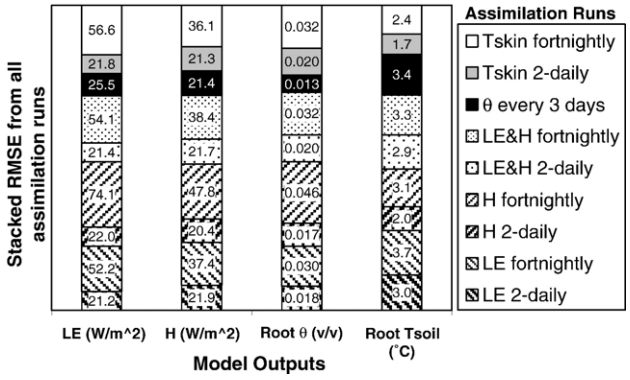

Fig. 6. RMSE values for the difference between assimilation and truth outputs of LE, H, root zone soil moisture (θ) and root zone soil temperature (T_{soil}) covering the 91 day experiment period from assimilating LE, H, surface soil moisture (θ) and skin temperature (T_{skin}) combinations.

the RMSE between the truth and all of the assimilation outputs for LE, H, root zone soil moisture and temperature. Of the heat flux and skin temperature assimilation experiments, assimilating twice a day (MODIS) achieves better retrieval of truth predictions than fortnightly assimilation (Landsat). This result is due to temporal resolutions; results may be different if spatial resolution effects are taken into account. The spatial resolution differs greatly between MODIS and Landsat, which have 1 km and 30 m pixels respectively. If there is significant heterogeneity at scales less than 1 km in the landscape, this would have potentially significant impacts on the assimilation accuracy.

Of the twice daily assimilations, the RMSE values indicate that LE assimilation achieves slightly better LE predictions than H assimilation and vice-versa. The root zone soil moisture predictions for LE assimilation are slightly worse than for H assimilation. Also evident is the considerably lower root zone soil temperature RMSE from H assimilation, as H is more closely related to soil temperature in the model formulation than LE. On the fortnightly time scale, LE assimilation results in better predictions for both LE and H, while also producing better root zone soil moisture predictions but poorer soil temperature than H assimilation. Comparing the individual LE and H assimilation results for the two time scales, LE assimilation produces the best LE results in both cases, and whichever assimilation produces the best soil moisture prediction also achieves the better H prediction; H assimilation achieves the best soil temperature in both cases as expected. Joint LE and H assimilation twice daily achieves similar improvements to both LE and H predictions compared with assimilation of each variable individually on a twice daily time scale. On a fortnightly scale, joint LE and H assimilation produces similar improvements in LE and H as fortnightly LE assimilation, and greater improvements than fortnightly H assimilation.

Assimilating surface soil moisture every 3 days resulted in poorer LE predictions than any of the twice daily heat flux assimilation experiments but had considerably lower RMSE for root zone soil moisture prediction than any other experiment, reinforcing the qualitative interpretations of the initial 6 days of assimilation shown in Fig. 5. Regarding H predictions, soil moisture assimilation produced outputs that have ~1–2% vol/vol lower RMSE than from twice per day joint LE and H, and LE assimilation, but higher RMSE than from twice per day H assimilation. When considering the spatial resolution of remotely sensed observation data available (~1 km × 1 km for LE and H from MODIS and ~50 km × 50 km for surface soil moisture from SMOS), assimilation of LE and/or H could potentially produce better overall heat flux predictions from a LSM such as the CBM for a period that is relatively cloud free, compared with soil moisture assimilation based on the results here. However, more detailed analyses are required for a range of different initial conditions, parameter inputs, temporal and spatial resolutions in order to show definitively that assimilating a particular variable can consistently produce better LE and H predictions.

The assimilation of skin temperature twice a day resulted in predicted heat flux accuracies that were very similar to those from twice daily heat flux assimilation experiments. Fortnightly skin temperature assimilation achieved similar predictions of LE and H to fortnightly LE and joint LE and H assimilation, and better predictions than fortnightly H assimilation. When compared with the heat flux assimilation experiments for corresponding time scales, skin temperature assimilation has a strong impact on improving root zone soil temperature, as shown by the small RMSE values.

The ability of skin temperature assimilation to match the predictive accuracy of heat fluxes from the heat flux assimilation experiments is likely to be related to the strong relationship that skin temperature has with the surface net radiation, which directly impacts on the surface energy balance and thus strongly influences both LE and H in the model. An interesting implication of these results is the apparent lack of benefit in assimilating LE and H estimates representing quantities that would be derived from remotely sensed skin temperature observations as compared to direct skin temperature assimilation. However, these results may be an artefact of how the LE and H estimates were derived in this synthetic study, as the same skin temperature — LE/H relationships are used in the assimilation as for LE and H observation generation, which will not be the case with actual remote sensing data. Therefore LE and H derived from real remotely sensed skin temperature using an algorithm (such as SEBAL) must be assimilated and compared with direct skin temperature assimilation to make definitive statements in this regard. A key question is whether an energy balance model such as SEBAL can provide better LE and H estimates than an LSM through skin temperature assimilation.

5. Conclusions

This paper has compared the assimilation impact of LE, H, skin temperature and surface soil moisture observations, representing typically available remotely sensed data and temporal repeat (MODIS, Landsat and SMOS), to understand the relative impact on LSM predictions of LE, H, root zone soil moisture and temperature, in a synthetic experiment framework. Soil moisture assimilation is the more traditional approach for

Please cite this article as: Pipunic, R. C. et al. Assimilation of remotely sensed data for improved latent and sensible heat flux prediction: A comparative synthetic study. *Remote Sensing of Environment* (2007), doi:10.1016/j.rse.2007.02.038

improving LSM predictions, and as expected, showed the most direct impact on root zone soil moisture. While it also improved heat flux predictions, the other approaches performed comparatively in terms of H predictions and slightly better in terms of LE predictions, when assimilated on a twice daily time scale, as these variables share more direct relationships with LE and H in the model. Moreover, they were able to have a direct impact on soil temperature predictions, which is not possible with direct soil moisture assimilation.

While this study clearly demonstrates that assimilation of LE and/or H has the potential to improve LE and H predictions to at least a similar degree as soil moisture assimilation, when tested under idealised conditions, the results may be different when cloud impacts and contrasting spatial resolutions are taken into consideration. Moreover, assimilating LE and H on a fortnightly temporal scale that is comparable to Landsat, resulted in significantly poorer LE and H predictions compared to twice daily LE and H assimilation that would be available from MODIS, and 3 day soil moisture assimilation that would be available from SMOS. This shows that if cloud cover reduces the temporal quality of remotely sensed LE and H observations (also of skin temperature), it can reduce the predictive performance of LE and H considerably. Hence, further research is required to make definitive conclusions regarding the best variables to assimilate for improved LE and H prediction. This includes assimilating over a range of different time scales, soil moisture conditions, soil and vegetation parameters, and using real remotely sensed observations so that the different spatial scales and error sources can be considered. Since LE and/or H, and skin temperature assimilation has shown promise for improving predictions of LE and H in these experiments, further field-based studies are warranted. Moreover, assimilation of a combination of the available data may provide the best results, complimenting the different spatial and temporal characteristics with the different land surface variables that are observed.

Acknowledgements

This work has been funded by a University of Melbourne–CSIRO Collaborative Research Support Scheme grant. The authors are grateful to Dr. Ying Ping Wang and Dr. Cathy Trudinger from CSIRO Marine and Atmospheric Research Division for supplying and permitting the use of CBM for this research and also providing valuable discussion on details of the model. Also Dr. Neil McKenzie from CSIRO Land and Water Division for supplying soils data. Dr. John Gorman from the Bureau of Meteorology assisted with queries relating to Bureau of Meteorology data used by this study. Robert Pipunic is supported by an Australian Postgraduate Award Scholarship.

References

Bastiaanssen, W. G. M., Menenti, M., Feddes, R. A., & Holtslag, A. A. M. (1998). A remote sensing surface energy balance algorithm for land (SEBAL) 1. Formulation. *Journal of Hydrology*, *213*, 198−212.

Bouttier, F., Mahfouf, J. F., & Noilhan, J. (1993). Sequential assimilation of soil moisture from atmospheric low-level parameters. Part I: Sensitivity and calibration studies. *Journal of Applied Meteorology*, *32*, 1352−1364.

Crosson, W. L., Laymon, C. A., Inguva, R., & Schamschula, M. P. (2002). Assimilating remote sensing data in a surface flux-soil moisture model. *Hydrological Processes*, *16*, 1645−1662.

Crow, W. T., & Wood, E. F. (2003). The assimilation of remotely sensed soil brightness temperature imagery into a land surface model using Ensemble Kalman filtering: A case study based on ESTAR measurements during SGP97. *Advances in Water Resources*, *26*, 137−149.

Entekhabi, D., Nakamura, H., & Njoku, E. G. (1994). Solving the inverse problem for soil moisture and temperature profiles by sequential assimilation of multifrequency remotely sensed observations. *IEEE Transactions on Geoscience and Remote Sensing*, *32*, 438−448.

Evensen, G. (1994). Sequential data assimilation with a nonlinear quasi-geostrophic model using Monte Carlo methods to forecast error statistics. *Journal of Geophysical Research — Oceans*, *99*, 10,143−10,162.

Franks, S. W., & Beven, K. J. (1999). Conditioning a multiple-patch SVAT model using uncertain time-space estimates of latent heat fluxes as inferred from remotely sensed data. *Water Resources Research*, *35*, 2751−2761.

French, A. N., Jacob, F., Anderson, M. C., Kustas, W. P., Timmermans, W., Gieske, A., et al. (2005). Surface energy fluxes with the Advanced Spaceborne Thermal Emission and Reflection radiometer (ASTER) at the Iowa 2002 SMACEX site (USA). *Remote Sensing of Environment*, *99*, 55−65.

Houtekamer, P. L., & Mitchell, H. L. (1998). Data assimilation using Ensemble Kalman filter techniques. *Monthly Weather Review*, *126*, 796−811.

Jiang, L., & Islam, S. (2001). Estimation of surface evaporation map over southern Great Plains using remote sensing data. *Water Resources Research*, *37*, 329−340.

Kaleita, A. L., & Kumar, P. (2000). AVHRR estimates of surface temperature during the Southern Great Plains 1997 Experiment. *Journal of Geophysical Research*, *105*, 20,791−20,801.

Kalman, R. E. (1960). A new approach to linear filtering and prediction problems. *Transaction of the ASME — Journal of Basic Engineering*, *82*, 35−45.

Kerr, Y. H., Waldteufel, P., Wigneron, J. -P., Martinuzzi, J. -M., Font, J., & Berger, M. (2001). Soil moisture retrieval from space: The Soil Moisture and Ocean Salinity (SMOS) mission. *IEEE Transactions on Geoscience and Remote Sensing*, *39*, 1729−1735.

Kowalczyk, E. A., Garrat, J. R., & Krummel, P. B. (1994). *CSIRO Division of atmospheric research technical paper 32.* Melbourne: CSIRO.

Kustas, W. P., & Norman, J. M. (1996). Use of remote sensing for evapotranspiration monitoring over land surfaces. *Hydrological Sciences Journal–Journal Des Sciences Hydrologiques*, *41*, 495−516.

Lu, H., Raupach, M. R., & McVicar, T. R. (2001). *CSIRO technical report 35/01.* CSIRO.

Mahfouf, J. F. (1991). Analysis of soil moisture from near surface parameters: A feasibility study. *Journal of Applied Meteorology*, *30*, 1534−1547.

Mahfouf, J. F., & Noilhan, J. (1991). Comparative study of various formulations of evaporation from bare soil using in situ data. *Journal of Applied Meteorology*, *30*, 1354−1365.

Margulis, S. A., & Entekhabi, D. (2003). Variational assimilation of radiometric surface temperature and reference-level micrometeorology into a model of the atmospheric boundary layer and land surface. *Monthly Weather Review*, *131*, 1272−1288.

Maybeck, P. S. (1979). *Stochastic models, estimation, and control.* New York: Academic Press, Inc.

McNider, R. T., Song, A. J., Casey, D. M., Wetzel, P. J., Crosson, W. L., & Rabin, R. M. (1994). Towards a dynamic thermodynamic assimilation of satellite surface temperature in numerical atmospheric models. *Monthly Weather Review*, *122*, 2784−2803.

Mertens, J., Madsen, H., Kristensen, M., Jacques, D., & Feyen, J. (2005). Sensitivity of soil parameters in unsaturated zone modelling and the relation between effective, laboratory and in situ estimates. *Hydrological Processes*, *19*, 1611−1633.

Pitman, A. J. (2003). The evolution of, and revolution in, land surface schemes designed for climate models. *International Journal of Climatology*, *23*, 479−510.

Raupach, M. R. (1989). A practical Lagrangian method for relating concentrations to source distributions in vegetation canopies. *Quarterly Journal of Royal Meteorology Society*, *115*, 609−632.

Please cite this article as: Pipunic, R. C. et al. Assimilation of remotely sensed data for improved latent and sensible heat flux prediction: A comparative synthetic study. *Remote Sensing of Environment* (2007), doi:10.1016/j.rse.2007.02.038

Reichle, R. H., Walker, J. P., Koster, R. D., & Houser, P. R. (2002). Extended versus Ensemble Kalman Filtering for Land Data Assimilation. *Journal of Hydrometeorology*, *3*, 728−740.

Schuurmans, J. M., Troch, P. A., Veldhuizen, A. A., Bastiaanssen, W. G. M., & Bierkens, M. F. P. (2003). Assimilation of remotely sensed latent heat flux in a distributed hydrological model. *Advances in Water Resources*, *26*, 151−159.

Seuffert, G., Wilker, H., Viterbo, P., Mahfouf, J. -F., Drusch, M., & Calvet, J. -C. (2003). Soil moisture analysis combining screen-level parameters and microwave brightness temperature: A test with field data. *Geophysical Research Letters*, *30*, 1498.

Siriwardena, L., Chiew, F., Richter, H., & Western, A. (2003). *Cooperative research centre for catchment hydrology.* Australia.

Sun, D., Pinker, R. T., & Basara, J. B. (2004). Land surface temperature estimation from the next generation of Geostationary Operational Environmental Satellites: GOES M-Q. *Journal of Applied Meteorology*, *43*, 363−372.

Turner, M. R. J., Walker, J. P., & Oke, P. R. (2006). Ensemble Member Generation for Sequential Data Assimilation. *Remote Sensing of Environment*, in press (this issue).

Walker, J. P., & Houser, P. R. (2001). A methodology for initializing soil moisture in a global climate model: Assimilation of near surface soil moisture observations. *Journal of Geophysical Research*, *106*, 11,761−11,774.

Walker, J. P., & Houser, P. R. (2005). In A. Aswathanarayana (Ed.), *Advances in water science methodologies* (pp. 230). Rotterdam: A.A. Balkema.

Wang, Y. -P., & Leuning, R. (1998). A two-leaf model for canopy conductance, photosynthesis and partitioning of available energy. I. Model description and comparison with a multilayered model. *Agricultural and Forest Meteorology*, *91*, 89−111.

Wang, Y. -P., Leuning, R., Cleugh, H. A., & Coppin, P. A. (2001). Parameter estimation in surface exchange models using nonlinear inversion: How many parameters can we estimate and which measurements are most useful? *Global Change Biology*, *7*, 495−510.

Yates, D. N., Chen, F., & Nagai, H. (2003). Land surface heterogeneity in the Cooperative Atmosphere Surface Exchange Study (CASES-97). Part II: Analysis of spatial heterogeneity and its scaling. *Journal of Hydrometeorology*, *4*, 219−234.

Please cite this article as: Pipunic, R. C. et al. Assimilation of remotely sensed data for improved latent and sensible heat flux prediction: A comparative synthetic study. *Remote Sensing of Environment* (2007), doi:10.1016/j.rse.2007.02.038